Received: 21 August 2018 | Revised: 5 April 2019 | Accepted: 8 April 2019

DOI: 10.1002/eco.2093

RESEARCH ARTICLE

WILEY

Ecosystem processes at the watershed scale: Influence of flowpath patterns of canopy ecophysiology on emergent catchment water and carbon cycling

Laurence Lin[1] | Lawrence E. Band[1,2] | James M. Vose[3] | Taehee Hwang[4] | Chelcy Ford Miniat[5] | Paul V. Bolstad[6]

[1] Department of Environmental Science, University of Virginia, Charlottesville, Virginia

[2] Department of Engineering Systems and Environment, University of Virginia, Charlottesville, Virginia

[3] Unites States Forest Service, Southern Research Station, Raleigh, North Carolina

[4] Department of Geography, Indiana University Bloomington, Bloomington, Indiana

[5] USDA FS SRS, Coweeta Hydrologic Laboratory, Otto, North Carolina

[6] Department of Forest Resources, University of Minnesota, St. Paul, Minnesota

Correspondence
Laurence Lin, Department of Environmental Science, University of Virginia, Charlottesville, VA 22903.
Email: hl8vq@virginia.edu

Funding information
NSF grants supporting the Coweeta Long Term Ecological Study, Grant/Award Number: DEB - 637522, DEB-1440484 and DEB-0823923, NSF Cybe; NSF, Grant/Award Numbers: NSF CyberSEES CCF-1331813, DEB-0823923, DEB-1440484 and DEB-637522

Abstract

Forest canopy water use and carbon cycling traits (WCT) can vary substantially and in spatially organized patterns, with significant impacts on watershed ecohydrology. In many watersheds, WCT may vary systematically along and between hydrologic flowpaths as an adaptation to available soil water, nutrients, and microclimate-mediated atmospheric water demand. We hypothesize that the emerging patterns of WCT at the hillslope to catchment scale provide a more resistant ecohydrological system, particularly with respect to drought stress, and the maintenance of high levels of productivity. Rather than attempting to address this hypothesis with species-specific patterns, we outline broader functional WCT groups and explore the sensitivity of water and carbon balances to the representation of canopy WCT functional organization through a modelling approach. We use a well-studied experimental watershed in North Carolina where detailed mapping of forest community patterns are sufficient to describe WCT functional organization. Ecohydrological models typically use broad-scale characterizations of forest canopy composition based on remotely sensed information (e.g., evergreen vs. deciduous), which may not adequately represent the range or spatial pattern of functional group WCT at hillslope to watershed scales. We use three different representations of WCT functional organizations: (1) restricting WCT to deciduous/conifer differentiation, (2) utilizing more detailed, but aspatial, information on local forest community composition, and (3) spatially distributed representation of local forest WCT. Accounting for WCT functional organization information improves model performance not only in terms of capturing observed flow regimes (especially watershed-scale seasonal flow dynamics) but also in terms of representing more detailed canopy ecohydrologic behaviour (e.g., root zone soil moisture, evapotranspiration, and net canopy photosynthesis), especially under dry condition. Results suggest that the well-known zonation of forest communities over hydrologic gradients is not just a local adaptation but also provides a property that regulates hillslope to catchment-scale behaviour of water use and drought resistance.

KEYWORDS

carbon cycling, ecohydrologic behaviour, ecosystem resistance, functional organization, water use, watershed

1 | INTRODUCTION

It is well established that different tree species vary in water use strategies and carbon assimilation based on physiological characteristics (e.g., xylem anatomy, stomatal conductance, and root architecture) and leaf display (e.g., Ford, Hubbard, & Vose, 2010; Ford, Laseter, Swank, & Vose, 2011; Pataki & Oren, 2003; Pataki, Oren, Katul, & Sigmon, 1998; Vose et al., 2016; Wolz, Wertin, Abordo, Wang, & Leakey, 2017). In terms of the regulation of water use, isohydric species such as red maple (*Acer rubrum*), tulip poplar (*Liriodendron tulipifera*), and evergreen trees with tracheid xylem including loblolly pine (*Pinus taeda*) have relatively high peak water use but reduce transpiration rapidly with decreasing atmospheric humidity to maintain leaf pressure. By comparison, anisohydric species, such as oaks (*Quercus* spp.), typically have lower peak water use but maintain transpiration rates as atmospheric humidity decreases (Ford et al., 2010; Ford et al., 2011; Klos, Wang, Bauerle, & Rieck, 2009; Vose et al., 2016). Forest community water use and carbon cycling traits (WCT), and subsequent response to water stress, can influence watershed-scale hydrologic behaviour by modifying hydrologic partitioning between evapotranspiration (ET) and surface/subsurface drainage flow patterns (Bosch & Hewlett, 1982; Jarvis & McNaughton, 1986; Running et al., 1989), in turn feeding back to patterns of available soil moisture and leaf area (Mackay & Band, 1997; Naithani, Baldwin, Gaines, Lin, & Eissenstat, 2013). In this study, we define the WCT functional organization as the spatial pattern of WCT along hillslope flowpaths. In the southern Appalachian Mountains and elsewhere, vegetation communities along hillslope flowpaths transition from a dominantly anisohydric community (e.g., oaks) upslope to a dominantly isohydric community (e.g., maples and poplars) downslope.

It has been hypothesized for decades that vegetation adapts to optimize water use efficiency at the patch scale (e.g., Eagleson, 1982). Beyond the patch scale, it is well known that forest communities are typically arranged along hydrologic gradients according to water use traits (e.g., Whittaker, 1956). We have previously shown that hillslope patterns of tree leaf area index (LAI) in southern Appalachian forests tend to increase along water flow paths at a rate proportional to the balance of water availability relative to atmospheric water demand, and in a manner that optimizes carbon assimilation and transpiration (Hwang, Band, & Hales, 2009; Hwang, Band, Vose, & Tague, 2012). This optimization is based, at least in part, on the release of moisture from upslope patches, subsidizing water and nitrogen availability to downslope communities (Hwang et al., 2009). The adjustment of leaf area with available water can manifest itself in a tight coupling of vegetation water use under dry conditions with low-flow dynamics (Bond et al., 2002). This provides a nonlocal property that downslope subsidy buffers the hillslope to catchment-scale ecosystem resistance to drought (Hawthrone & Miniat, 2016).

In this study, we extend our prior research by investigating the role of WCT functional organization, in addition to canopy structural properties, in hillslope to catchment-scale emergent water and carbon cycling behaviour. We pose two research questions to investigate the importance of WCT functional organization in regulating catchment-scale ecohydrologic processes and catchment to drought:

1. How does emergent catchment streamflow and hillslope ecohydrological behaviour vary in response to different forms of WCT functional organization?
2. How is the downslope subsidy expressed under different hydroclimate conditions with different levels of WCT functional organization, and how does it influence forest ecosystem resistance to drought?

We hypothesize that (a) forest functional WCT has an important influence on hillslope to catchment hydrological behaviour, maintaining higher levels of ecosystem ET and productivity, and (b) better expressed (more organized) WCT functional organization increases hillslope to catchment resistance to drought stress. We use the Regional Hydro-Ecologic Simulation System (RHESSys) to investigate these questions by simulating the interactions and feedbacks between landscape ecological and hydrologic processes with different forms of WCT functional organization specified. Specifically, we design three different scenarios ranging from low to high levels of canopy WCT functional organization representation in terms of the site specific and spatial organization of canopy structure and ecophysiologic behaviour along hydrologic flowpaths. We then use RHESSys simulation to investigate how these three levels of WCT functional organization affects both landscape patterns and emergent catchment-scale ecohydrologic processes. In particular, we examine the effect of WCT functional organization on ET, productivity (e.g., net canopy photosynthesis and PSN), rootzone saturation and soil water dynamics, and the effect on model performance in capturing observed streamflow patterns, particularly over interannual and seasonal cycles, and low flow under dry conditions.

2 | METHODS

2.1 | Study watershed

Our study watershed is watershed 18 (WS18) at the Coweeta Hydrologic Lab, NC, a National Science Foundation funded Long-Term Ecological Research site and a U.S. Forest Service Experimental Forest. WS18 has been well studied with long-term stream discharge, climate data, soil moisture, and forest community inventory and mapping (Figure 1). The Coweeta watersheds are characterized by high biodiversity, strong topographic, and climatic gradients. Catchment discharge, meteorology, and spatial vegetation patterns have been measured since the 1930s, including permanent plots and remote sensing data to estimate leaf area, vegetation community, and species composition. WS18 is a control watershed with mixed hardwood stands and has remained undisturbed by human activity since 1927. Average annual rainfall at the central meteorological station in the Coweeta valley is 1,880 mm, evenly distributed throughout the year. Annual run-off ratios range from 48–75% varying with interannual

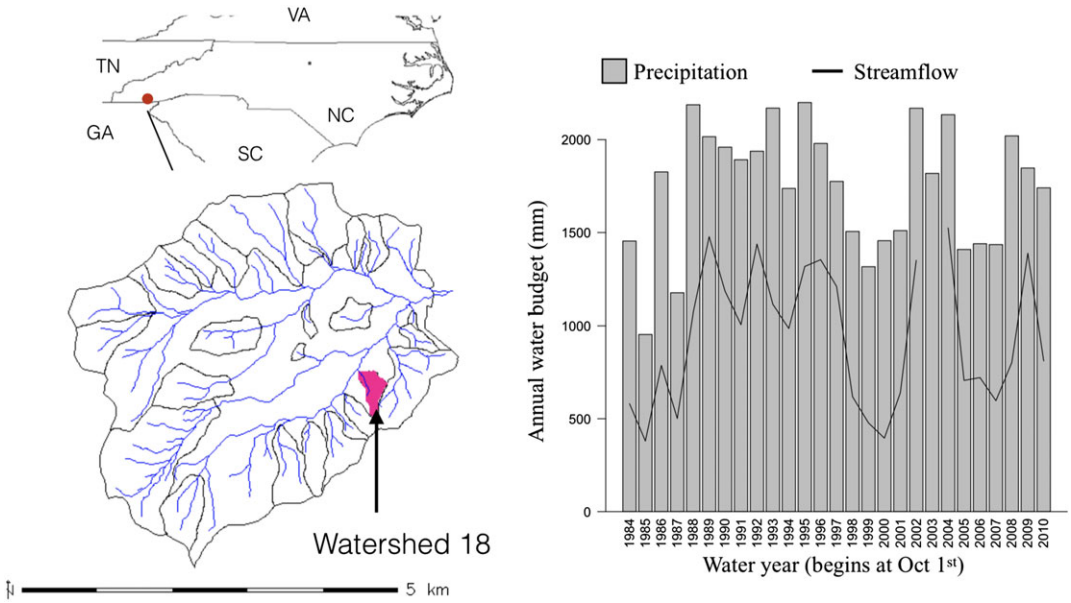

FIGURE 1 Watershed 18 (WS18) within Coweeta Basin, NC, as well as annual precipitation and streamflow in WS18

climate (Swift, Cunningham, & Douglass, 1988) but have shown a decreasing trend over the last few decades (Caldwell et al., 2016). Mean monthly temperatures range from 4.6°C in winter to 20.7°C in summer (Laseter, Ford, Vose, & Swift, 2012). Forest tree community and species distribution in the Coweeta Basin have been mapped and described by several earlier studies (Bolstad, Swank, & Vose, 1998; Braun, 1950; F. Day, Phillips, & Monk, 1988; F. P. Day & Monk, 1974; Elliott & Vose, 2011; Eyre, 1980; Whittaker, 1956). The dominant forest types range from more dominantly oak (*Quercus* spp.) and hickory (*Carya* spp.) at upper slopes, to tulip poplar (*L. tulipifera*), sweet birch (*Betula lenta*), and eastern hemlock (*Tsuga canadensis*) at wetter, downslope coves (Bolstad et al., 1998; Elliott & Vose, 2011; Elliott, Vose, Swank, & Bolstad, 1999), although the hemlock canopy was recently eliminated by invasive infestation by woolly adelgid (Ford, Elliott, Clinton, Kloeppel, & Vose, 2012). The understorey shrub layer is primarily comprised *Rhododendron maximum* (F. Day et al., 1988; Elliott & Vose, 2012) with more limited occurrence of mountain laurel (*Kalmia latifolia*). Vegetation rooting depths by tree species related to species and topographic locations were also studied within the Coweeta Basin (Hales, Ford, Hwang, Vose, & Band, 2009; McGinty, 1976). Despite high rainfall, soil water availability plays a significant role influencing vegetation patterns within WS18, with topographically driven drainage on steep slopes with colluvial soils mostly via shallow subsurface flow (F. P. Day & Monk, 1974; Hewlett & Hibbert, 1963) leading to strong hillslope scale zonation of soil water during dry periods. WS18 has an increasing spatial gradient in leaf area from ridge to hollow (Hwang et al., 2009; Hwang et al., 2012).

2.2 | Regional Hydro-Ecologic Simulation System

RHESSys couples elements of the ecosystem models BIOME-BGC (Running & Hunt, 1993) and CENTURY (Parton, Schimel, Cole, & Ojima, 1987), with distributed watershed models to derive the coupling between ecosystem water use, carbon and nitrogen cycling with lateral soil water redistribution. RHESSys has been widely used to estimate spatially distributed soil moisture, ET, surface and subsurface run-off, carbon and nitrogen cycling in different biomes and under different climate and land use change scenarios (e.g., Band, Patterson, Nemani, & Running, 1993; Bart, Tague, & Moritz, 2016; Garcia, Tague, & Choate, 2016; Hanan, Tague, & Schimel, 2017; Hwang et al., 2009; Lin, 2013; Lin, Webster, Hwang, & Band, 2015; Miles & Band, 2015; Tague & Band, 2004). RHESSys uses a landscape hierarchical structure over nested patch (Figure 2), hillslope and watershed scales (Figure 3).

In the model application used here, we use a lateral drainage approach drawn from the Distributed Hydrology Soil Vegetation Model (Wigmosta, Vail, & Lettenmaier, 1994) for surface and shallow

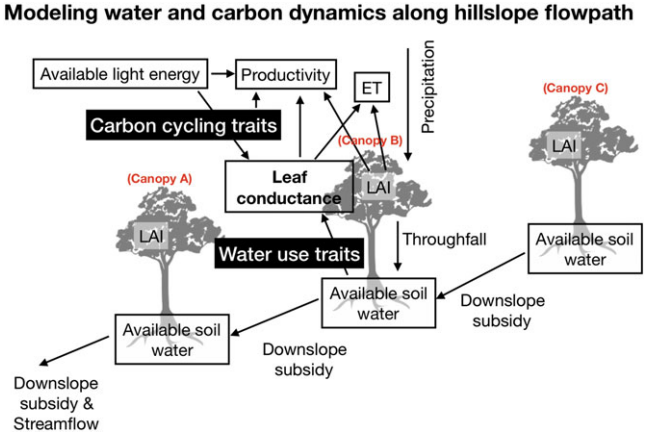

FIGURE 2 A conceptual figure showing the roles of water use and carbon cycling traits in forest productivity, leaf conductance, and evapotranspiration. Water use and carbon cycling traits are as important as LAI to characterize catchment canopy and could have influences to soil water and streamflow generation in the model. ET, evapotranspiration; LAI, leaf area index

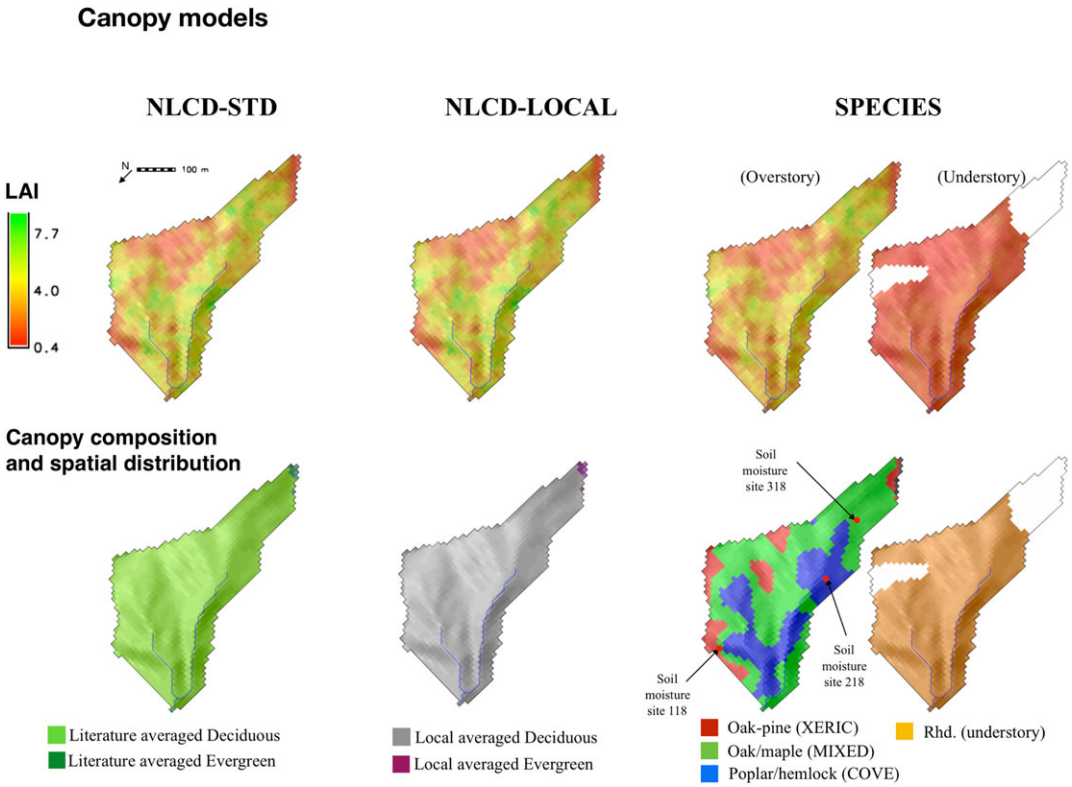

FIGURE 3 The leaf area index (LAI), the forest set-up based on the National Land Cover Database (NLCD-STD and NLCD-LOCAL models) and the forest set-up based on diverse tree species information (SPECIES model) for Watershed 18 (WS18). The total LAI was based on a remote sensing study (Hwang et al., 2009). The overstorey LAI was estimated according to a LAI ratio of Rhododendron (Rhd.): overstorey that varies by distance to stream (Elliott & Vose, 2012). The vegetation composition was based on Bolstad et al. (1998). The figure also shows three observed sites (red dots) within WS18 that are located at COVE, MIXED, and XERIC, respectively. Rootzone depth was estimated by tree species allometric relationship in SPECIES model; by weighted averaged allometric relationship in NLCD-LOCAL; and by basin average in NLCD-STD (see Table 1 for details)

subsurface flow from ridge to stream, and route a conceptual deep groundwater storage outflow to lower slope and riparian zones (approximated by less than 20 m flow distance to the observed channels) rather than directly to streams, with Van Genuchten soil water characteristics (Van Genuchten & Nielsen, 1985). The canopy is parameterized from empirical measurements (e.g., LAI, vegetation type, canopy structural characteristics, and ecophysiological traits). Vegetation phenology and canopy ecohydrologic processes are simulated, but interannual canopy changes in LAI and vegetation type are not included in this study. Other inputs of the model include soils, elevation, land use, and climate (i.e., precipitation and temperature). Water–carbon–nitrogen coupling is represented in the stomatal physiology, carbon assimilation and allocation (Dickinson, Shaikh, Bryant, & Graumlich, 1998, for deciduous and Waring, Landsberg, & Williams, 1998, for evergreen), and hydrologic processes using parameter libraries of WCT, enabling us to incorporate different levels of canopy WCT functional organization information in the model (described below). Details on the development of RHESSys can be found in Band et al. (1993) and Tague and Band (2004). Code and details on implementation are available at https://github.com/RHESSys/RHESSys.

Daily climate data for WS18 were obtained from the main meteorological station at the Coweeta Hydrologic Laboratory (Climate station CS01/RG06; http://coweeta.uga.edu). We extracted elevation data from a North Carolina state-wide LIDAR-based Elevation Data (www.lib.ncsu.edu/gis/elevation.html) and the soils data from the Natural Resources Conservation Service's Soil Survey Geographic Database. Additional land cover information were extracted from the 2011 National Land Cover Database (NLCD; Homer et al., 2015; U. S. Geological Survey), with more detailed information derived from multiple field based studies in Coweeta (Bolstad et al., 1998; Elliott & Vose, 2012). LAI values were calculated from field measurement and remote sensing data as reported in Hwang et al. (2009).

2.3 | Incorporating forest WCT functional organization into RHESSys

We developed three models for WS18 to represent varying details of compositional and spatial organization of patch canopy WCT. In these models, each grid cell (10 × 10 m) in the model represents a forest patch (referred as "forest patch" hereafter) and is assigned a LAI value (Hwang et al., 2009). RHESSys simulations a canopy–soil ecosystem model at each forest patch, with all patches connected along hydrologic flowpaths by the DHSVM routing (Table 1; Figure 2). In the first model using a standard biome classification (NLCD-STD), each forest patch was either deciduous or evergreen according to National Land Cover Dataset

TABLE 1 Three candidate models, including two models with a forest set-up based on the National Land Cover Database (NLCD-STD and NLDC-LOCAL) and the one based on diverse tree species information (SPECIES)

Model feature	Canopy representation in each forest patch	Model parameters for WCT	Vegetation rooting depth	LAI pattern
NLCD-STD	Deciduous or evergreen	Average of literature values across North America	Spatially constant; basin average	Spatially varying based on remote sensing
NLCD-LOCAL	Deciduous or evergreen	Weighted average based on dominant tree species in Coweeta Basin; no spatial patterns	Spatially varying (base on LAI pattern and weighted average allometric relationship)	Spatially varying based on remote sensing
SPECIES	Several dominant tree species; overstorey and understorey (shrub) canopy	Based on dominant tree species in Coweeta Basin; spatial patterns	Spatially varying (based on LAI pattern and tree species-specific allometric relationship)	Spatially varying based on remote sensing; divided into overstorey and understorey LAI

Abbreviations: LAI, leaf area index; WCT, water use and carbon cycling traits.

classification. We assumed no species- or community-specific vegetation composition, and no overstorey/understorey forest structure in each patch, but only generalized deciduous or evergreen vegetation. In NLCD-STD, the WCT parameter values (Data S1; standard deciduous and standard evergreen columns) were the most generalized as drawn from literature for deciduous or evergreen (White et al., 2000). The WCT parameter values for all deciduous patches in the study area were the same and so were the values for all evergreen patches. Vegetation rooting depth was set constant over space, as an estimated Coweeta Basin average (Hales et al., 2009; McGinty, 1976).

In the second model (NLCD-LOCAL), limited to overstorey canopy (no understorey), similar to NLCD-STD, but we assumed each deciduous or evergreen patch was composed of several dominant tree species (Data S1) determined from observations in Coweeta Basin. The WCT parameter values (Data S1; local deciduous and local evergreen columns) for each deciduous or evergreen patch in NLCD-LOCAL model aggregated from the composition of the dominant tree species but not spatially differentiated across the landscape. Vegetation rooting depth varied spatially based on the LAI pattern and a weighted average allometric relationship as described in Hwang et al. (2015).

The third model (SPECIES) incorporated WCT functional organization along topographic gradients. In the SPECIES model, we assumed each forest patch contained multiple tree species and overstorey/understorey forest structure. Remotely sensed LAI in each forest patch (Hwang et al., 2009) was divided into overstorey and understorey LAI based on Elliott and Vose (2012). In the Coweeta Basin, Rhododendron (*R. maximum*) is the dominant understorey vegetation. Mountain laurel (*K. latifolia*) is more prevalent in drier portions of the watershed but shows much lower percent ground cover than Rhododendron and, by contrast, was not well predicted by terrain analysis (Narayanaraj, Bolstad, Elliott, & Vose, 2010). In this version, we modelled all understorey as Rhododendron due to limited data for mountain laurel. The SPECIES model incorporates three overstorey vegetation communities, namely, oak-pine (xeric ridge and upper slopes), mixed deciduous (midslope), and cove (lower slopes, hollows) assemblages. We used poplar and hemlock to represent cove vegetation species and divided the forest patches of this zone into poplar and hemlock based on their basal area ratios available forest plot mensuration (Bolstad et al., 1998; F. Day et al., 1988). We note that hemlock was largely extirpated by woolly adelgid in Coweeta (Narayanaraj et al., 2010; Webster et al., 2012), with infestation starting about 2003. However, significant decline did not occur until 2008, and hemlock was a minor component in WS18. The mixed deciduous zone was dominated by spatially intermixed oak and red maple. We used a weighted average of the WCT parameters (Data S1; chestnut oak and red maple) between these two hardwood species to represent patch WCT; the weights used in calculating the weighted average were based on the basal area ratio of these two species (Bolstad et al., 1998; F. Day et al., 1988). We used oak to represent the xeric oak-pine zone as pine typically occupies only the most xeric or heavily disturbed sites in low elevation, north facing watersheds and is a small fraction of the overall vegetation. In the SPECIES model, spatial pattern of overstorey vegetation was derived on the basis of terrain characteristics, including elevation, slope, aspect, and terrain shape, following Bolstad et al. (1998). In the model, vegetation rooting depth varied spatially and varied across vegetation species functional groups based on LAI and vegetation allometric relationships (Hwang et al., 2015).

2.4 | Model calibration and comparison

We used observed daily streamflow data from 1990 to 2000 for calibration and data from 2001 to 2010 for validation to take advantage of the wide range in dry to wet conditions over the two decades. We calibrated each of the three models separately by maximizing a joint probability:

$$\begin{aligned}\text{Joint probability} = {} & f_1\left(1 - NSE_{\text{daily}} | 0.2\right) f_1\left(1 - NSE_{\text{log-daily}} | 0.2\right) \\ & f_1\left(1 - NSE_{\text{weekly}} | 0.2\right) f_1\left(1 - NSE_{\text{log-weekly}} | 0.2\right) \\ & f_1\left(1 - NSE_{1/\text{weekly}} | 0.2\right) f_1\left(1 - NSE_{\text{monthly}} | 0.2\right) \\ & f_2(|\,\text{annual bias}\| 0.2,\, 1),\end{aligned}$$

where *NSE* is Nash–Sutcliffe efficiencies, f_1 is the probability density function of an exponential distribution, and f_2 is the probability

density function of a Gamma distribution. NSE of inverse weekly flow (1/weekly flow) is calculated to further assess how well the model predicts low-flow patterns. Exponential and Gamma distribution functions were used to convert the NSE fitness measures into the joint probability for parameter search (see below). Separate calibrations for each model were used to emphasize different structural components (i.e., composition and distribution of vegetation types and water use trait parameterization) and the goal of distinguishing between model structure rather than parameter calibration. Model soil hydrological parameters: vertical and horizontal hydraulic conductivity, percentage bypass recharge, and storage dependent discharge rates of deep groundwater were calibrated through Markov chain Monte Carlo simulations (Gilks, Richardson, & Spiegelhalter, 1995). We ran a total of 5,000 simulation runs for each model. The 100 best model realizations were selected in each watershed and canopy setting for the analyses in this study.

In addition to evaluation of streamflow predictions, we also compared models with observations for rootzone saturation (%) with observed soil moisture in different topographic positions to further evaluate model performance. Simulated rootzone soil moisture content was compared with observed soil moisture dynamics from 0 to 60 cm soil depths at three sites in WS18, available since 1999, in upper slope (site 118), midslope (site 318), and riparian (site 218) plots (Figure 3; https://coweeta.uga.edu/dbpublic/dataset_details.asp?accession=1023). We used the correlation coefficient between daily simulated and observed rootzone soil moisture rather than the NSE for goodness of fit as the observed TDR depth is shallower than the simulated root zones in the RHESSys model.

We examined the influence of varying levels of canopy WCT functional organization and the influence of incorporating WCT spatial patterns on the landscape pattern of ET (mm) with soil moisture as key water balance components for the different vegetation community zones. We examined the monthly simulated pattern of ET, LAI, net canopy photosynthesis (PSN = Gross Primary Production − Maintenance Respiration, g C/m^2/month) and rootzone saturation (%) at three different landscape positions for a dry year (1999) and a wet year (2002) for each model. We here name three landscape positions according to the three vegetation zones defined in the SPECIES model, that is, the COVE position refers to the lower slopes and hollows; the MIXED position refers to midslope; and the XERIC position refers to the upper slopes and ridges. Lastly, we compared models in terms of their predictions of leaf conductance (m s^{-1}) and net soil water (NSW; defined as growing season patch scale precipitation—ET; mm) during growth seasons in dry (1999) and wet years (2002) to observe patterns of patch water use relative to precipitation in different landscape positions, as influenced by local patch properties and downslope subsidy.

3 | RESULTS

3.1 | Predicted streamflow

All three models achieved good fits to the discharge data through calibration, with SPECIES model performing slightly better compared with NLCD models during the calibration period and during the validation period (Table 2; Figure 4a–d). All models tended to overestimate streamflow through much of the dormant season (February–April during calibration period), and the two NLCD models underestimate flow during the growing season (May–October during calibration period; Figure 4c). However, the SPECIES model better captured observed winter flow and low-flow regimes (Figure 4c). For the validation period, all models have reasonable predictive power for streamflow (Table 2; Figures 4e–h). During dry (Figure 4f) and wet years (Figure 4g), such as 1999 (dry; Figure 1) and 2002 (wet), respectively, all models predict the seasonal trend of streamflow, but the SPECIES model performed better, most notably during the dry year growing season (Figure 4f). The annual total watershed ET estimated by the three models is 54.4%, 52.8%, and 55.2% of annual precipitation in the dry year (1999), and 37.4%, 33.4%, and 34.0% in the wet year (2002), for NLCD-STD, NLCD-LOCAL, and SPECIES, respectively. Plots of streamflow prediction (i.e., daily NSE) and soil moisture patterns (i.e., the correlation between model predicted and observed soil moisture) at the gradient plots (sites 118, 218, and 318) within WS18 by all three models follow a positive trend with explanatory power for both streamflow and soil moisture generally increasing from NLCD-STD, NLCD-LOCAL to SPECIES (Figure 4h).

TABLE 2 The Nash–Sutcliffe efficiencies (NSE) and the bias of the candidate models for Watershed 18

Candidate model	Daily NSE (log scale)	Weekly NSE (log scale)	Monthly NSE	Bias	NSE of (1/weekly flow)
Calibration period (1990–2000)					
NLCD-STD	0.83 ± 0.013 (0.89 ± 0.012)	0.91 ± 0.01 (0.91 ± 0.011)	0.94 ± 0.005	0.01 ± 0.007	0.74 ± 0.045
NLCD-LOCAL	0.84 ± 0.007 (0.89 ± 0.014)	0.92 ± 0.006 (0.91 ± 0.014)	0.95 ± 0.004	0.04 ± 0.027	0.77 ± 0.064
SPECIES	0.84 ± 0.002 (0.90 ± 0.006)	0.92 ± 0.002 (0.92 ± 0.005)	0.96 ± 0.002	0.03 ± 0.01	0.80 ± 0.04
Validation period (2001–2010)					
NLCD-STD	0.79 ± 0.017 (0.9 ± 0.012)	0.87 ± 0.013 (0.92 ± 0.012)	0.93 ± 0.006	−0.02 ± 0.007	0.86 ± 0.032
NLCD-LOCAL	0.81 ± 0.011 (0.89 ± 0.018)	0.89 ± 0.008 (0.91 ± 0.022)	0.94 ± 0.009	0.01 ± 0.028	0.76 ± 0.114
SPECIES	0.82 ± 0.004 (0.89 ± 0.004)	0.89 ± 0.003 (0.91 ± 0.006)	0.94 ± 0.003	−0.01 ± 0.011	0.82 ± 0.016

Note. The table shows the average from the top 100 best-fit models (refer to Table 1 for explanation of the three candidate models).

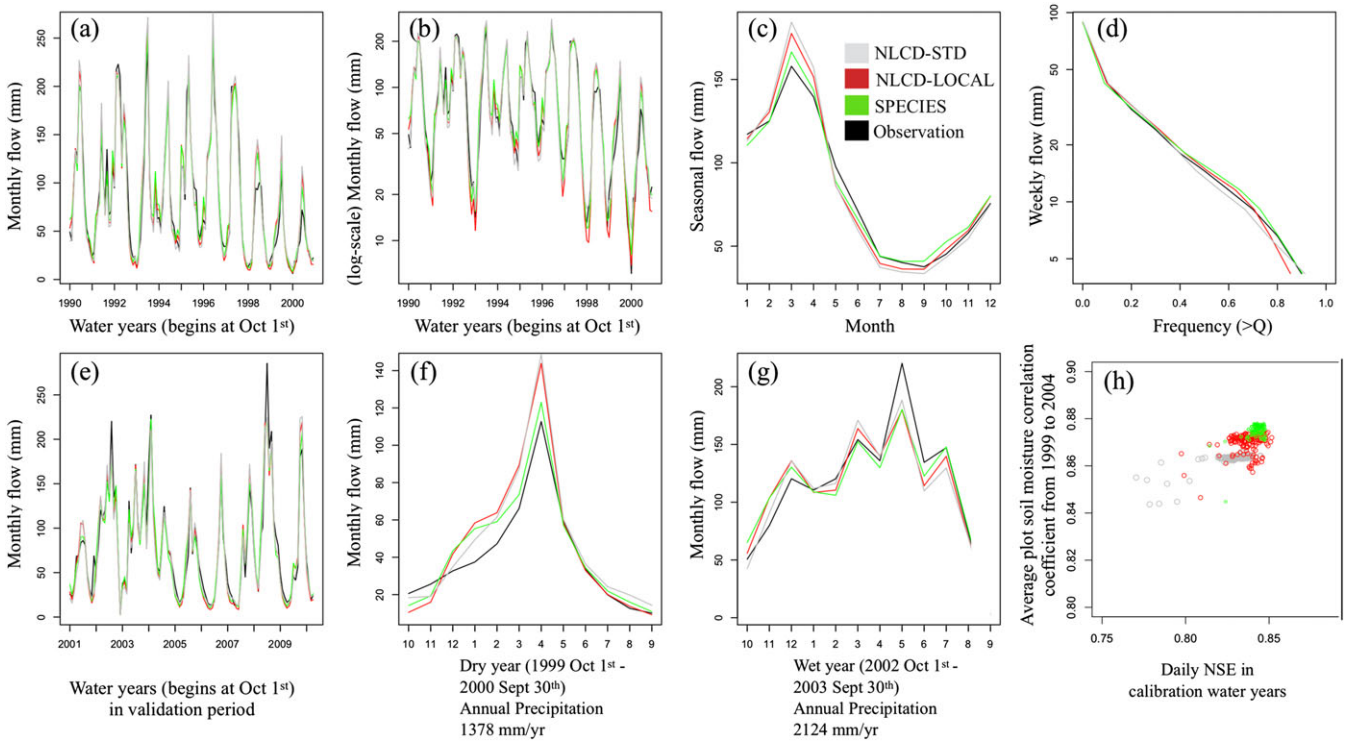

FIGURE 4 (a,b) Monthly (log) flow, (c) seasonal flow, (d) weekly flow duration curves that is observed at Watershed 18 and are generated by the three candidate models during calibration period (1990–2000), (e) monthly flow in validation period (2001–2010), (f,g) monthly flow in a dry year (1999) and a wet year (2002), and (h) average plot soil moisture correlation (COR) by daily NSE of the three candidate models. Refer to Table 1 for the explanation of candidate models. NSE, Nash–Sutcliffe efficiencies

3.2 | Seasonal and landscape patterns in ET, LAI, PSN, and rootzone saturation

The three models had similar LAI spatial patterns during growth season, with the highest LAI at cove and the lowest at xeric (Figure 5a–c) because we used the same spatial distribution of LAI in all three models. The zonation of both overstorey and understorey evergreen species contributes to higher dormant season cove LAI and ET in the SPECIES model compared with the two NLCD models (Figure 5c).

In a wet year (2002), ET at COVE and MIXED are higher than at XERIC for all models (Figure 5d–f). PSN is similar across landscape positions in the two NLCD models but more differentiated in the SPECIES model (Figure 5g–i). COVE has the highest estimated rootzone saturation (%) in all models, followed by MIXED and XERIC for NLCD-LOCAL and SPECIES models (Figure 5j–l).

Compared with a wet year, in a dry year (1999), LAI remains similar but ET, PSN, and rootzone saturation from mid spring to the beginning of fall (May–September) reduce substantially in all landscape positions (Figure 6j–l). During this period, the SPECIES model ET and PSN patterns diverge substantially above the two NLCD models. The SPECIES model COVE ET and PSN are the highest, followed by MIXED and XERIC, consistent with landscape patterns in SPECIES model in a wet year (Figures 5i and 6i) but are much more pronounced. ET shows little difference across landscape positions in NLCD-STD model (Figure 6d), and less difference across landscape positions in NLCD-LOCAL (Figure 6e) than in SPECIES (Figure 6f) model. The PSN at COVE and MIXED in the two NLCD models collapse as the growing season progresses and become less than XERIC from July to September (Figure 6g,h). The three models produce different landscape patterns in rootzone saturation. In the SPECIES model, COVE has the highest rootzone saturation year around, and rootzone saturation at MIXED and XERIC are similar (Figure 6i). The landscape pattern of rootzone saturation in the NLCD-LOCAL model is similar to SPECIES model except that rootzone saturation at MIXED becomes lower than XERIC during May to September (Figure 6k,l). In the NLCD-STD model, rootzone saturation at both COVE and MIXED drops below XERIC during May to Sept (Figure 6j).

The rootzone soil moisture simulated by all three models was highly correlated with the observed soil moisture at the three sites (i.e., one site at each landscape position; the averaged from multiple TDR readings was used for each site), with correlation coefficients ranging from 0.84 to 0.89 (Figure 7a–i). However, in some cases (e.g., summer in 2000–2002 in Figure 7a and summer in 2000 in Figure 7b), the two NLCD models predicted lower soil moisture content at the COVE site even with deeper COVE rootzone depths (i.e., 1.2 m) at which we expect higher soil moisture than at shallower depth (i.e., 0–60 cm observed measurement).

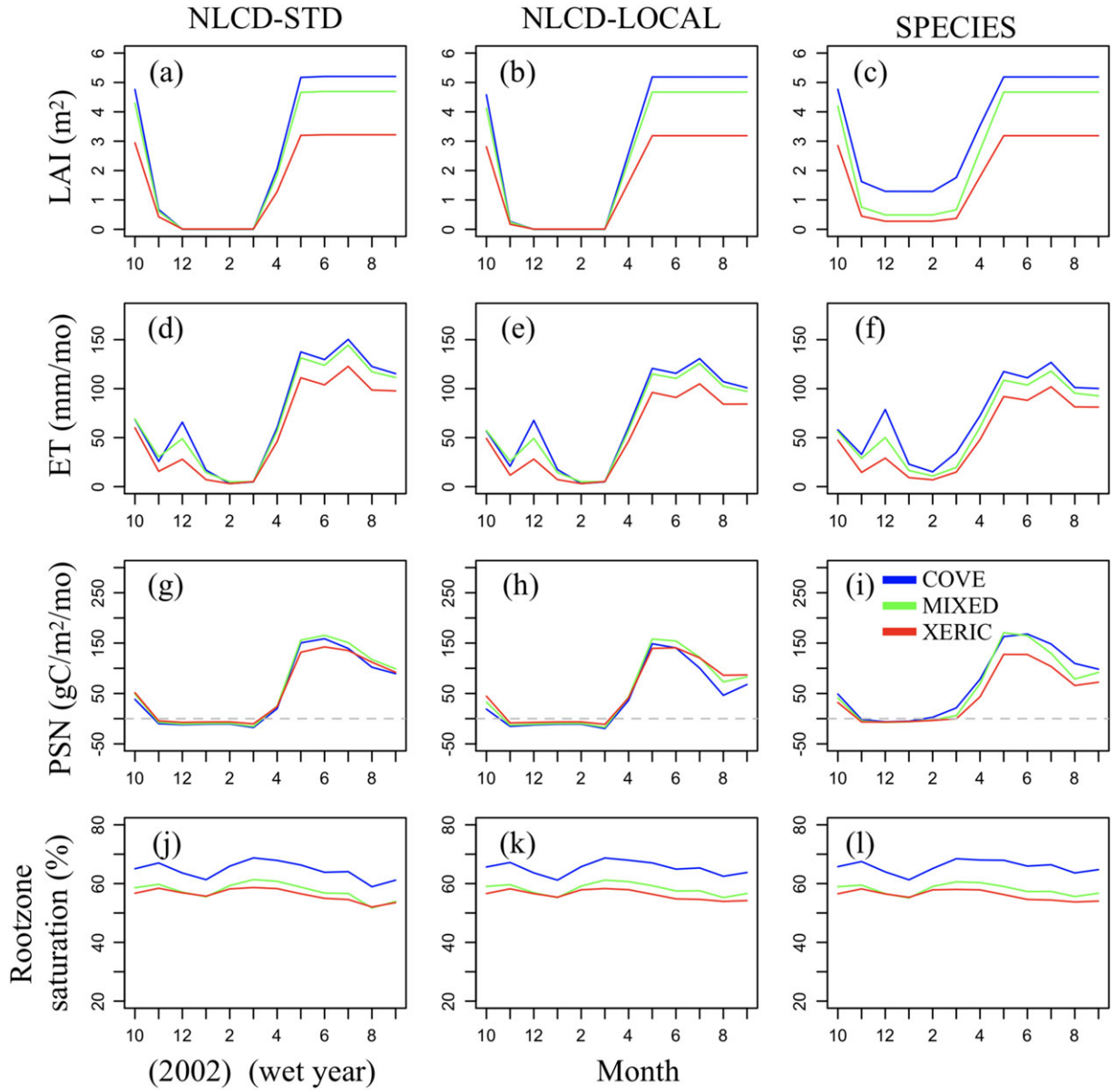

FIGURE 5 Monthly pattern of evapotranspiration (ET, mm), leaf area index (LAI, m^2), Photosynthesis Net (PSN = Gross Primary Production – Maintenance Respiration, g C/m^2/month), and rootzone saturation (%) at different landscape positions (i.e., COVE, MIXED, and XERIC) in a dry year (1999) at the Watershed 18, generated by the three candidate models. Refer to Table 1 for the explanation of candidate models

3.3 | Predicted spatial pattern in growing season NSW and leaf conductance

The patch NSW (pcp–ET) is evidence of downslope subsidy of soil water when its value is negative (ET > pcp). When positive, NSW represents precipitation in excess of local ET, providing surplus exported downslope and to streams. Upslope and midslope areas in SPECIES yield the most surplus downslope (Figure 8c,f), followed by the NLCD-LOCAL (Figure 8b,e) and the NLCD-STD (Figure 8a,d) models, under both wet and dry conditions. In the wet year, the whole catchment has positive NSW in all models. A general pattern emerges: upslope NSW is higher than downslope, with NSW sharply lower in dry years. In a dry year, a strong downslope subsidy is reflected by a more negative NSW value with NLCD-STD model having the lowest NSW in restricted areas immediately proximal to streams. NSW value sharply increases but remains negative (value near zero) just upslope of the channels and persists to the top of hillslopes where some precipitation surplus signals emerge (Figure 8d). The NSW pattern in NLCD-LOCAL is similar to that in NLCD-STD model except that the bottomland NSW values are more diffuse, and the positive NSW area upslope is wider (Figure 8e). SPECIES shows positive NSW in midslope areas and wider areas of negative NSW in the lower slopes (Figure 8f).

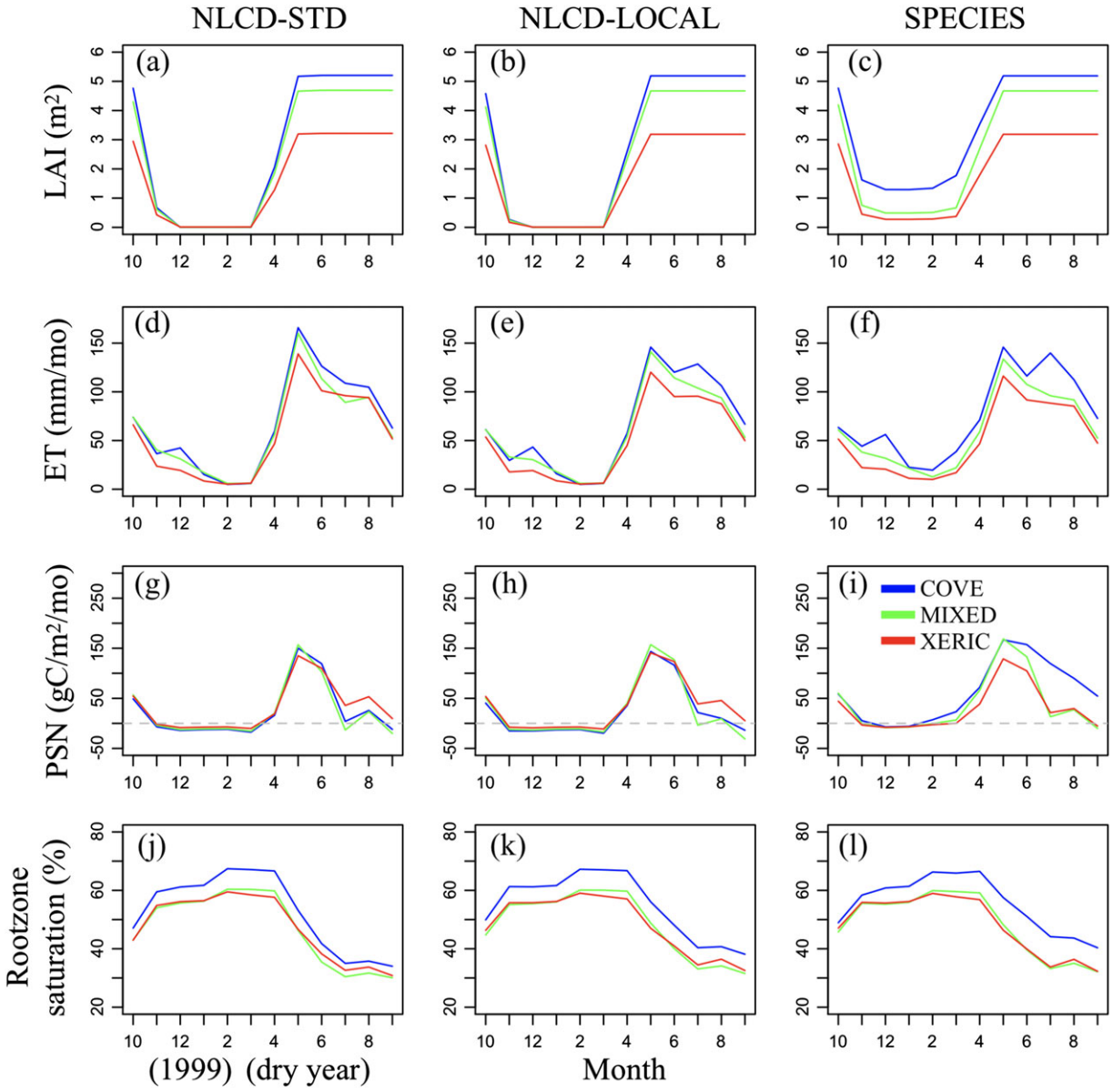

FIGURE 6 Monthly pattern of evapotranspiration (ET, mm), leaf area index (LAI, m^2), Photosynthesis Net (PSN = Gross Primary Production − Maintenance Respiration, g C/m^2/month), and rootzone saturation (%) at different landscape positions (i.e., COVE, MIXED, and XERIC) in a wet year (2002) at the Watershed 18, generated by the three candidate models. Refer to Table 1 for the explanation of candidate models

Differences in NSW patterns between models become more obvious when aggregating NSW value by landscape positions (Table 3). SPECIES has the lowest average NSW at COVE, that is, the most subsidy to downslope, followed by NLCD-LOCAL and NLCD-STD. SPECIES has precipitation surplus in MIXED, whereas the NLCD models show downslope subsidy in MIXED. SPECIES has the highest moisture surplus in XERIC, followed by NLCD-LOCAL and NLCD-STD. Additional useful information is the modelled leaf conductance (Table 4). By comparing the averaged leaf conductance by zones between wet and dry years, NLCD-STD has the highest percent leaf conductance reductions, followed by NLCD-LOCAL and SPECIES. Additionally, the percent reduction is higher in the MIXED than in COVE and XERIC in NLCD-LOCAL and SPECIES models (Table 4).

4 | DISCUSSION

4.1 | Forest WCT organization influence on streamflow and ecohydrological trends

All three models fit both run-off and soil moisture reasonably well based on fitness criteria (i.e., NSE and bias for run-off and correlation for soil moisture) as they were separately calibrated to the same streamflow data. In mountainous watersheds, many ecohydrologic traits covary spatially with landscape position and hydrologic flowpath (Band et al., 1993; Harmon, Bratton, & White, 1984; Mackay & Band, 1997; Naithani et al., 2013; Whittaker, 1956). The models that account for this covariation should be expected to perform better

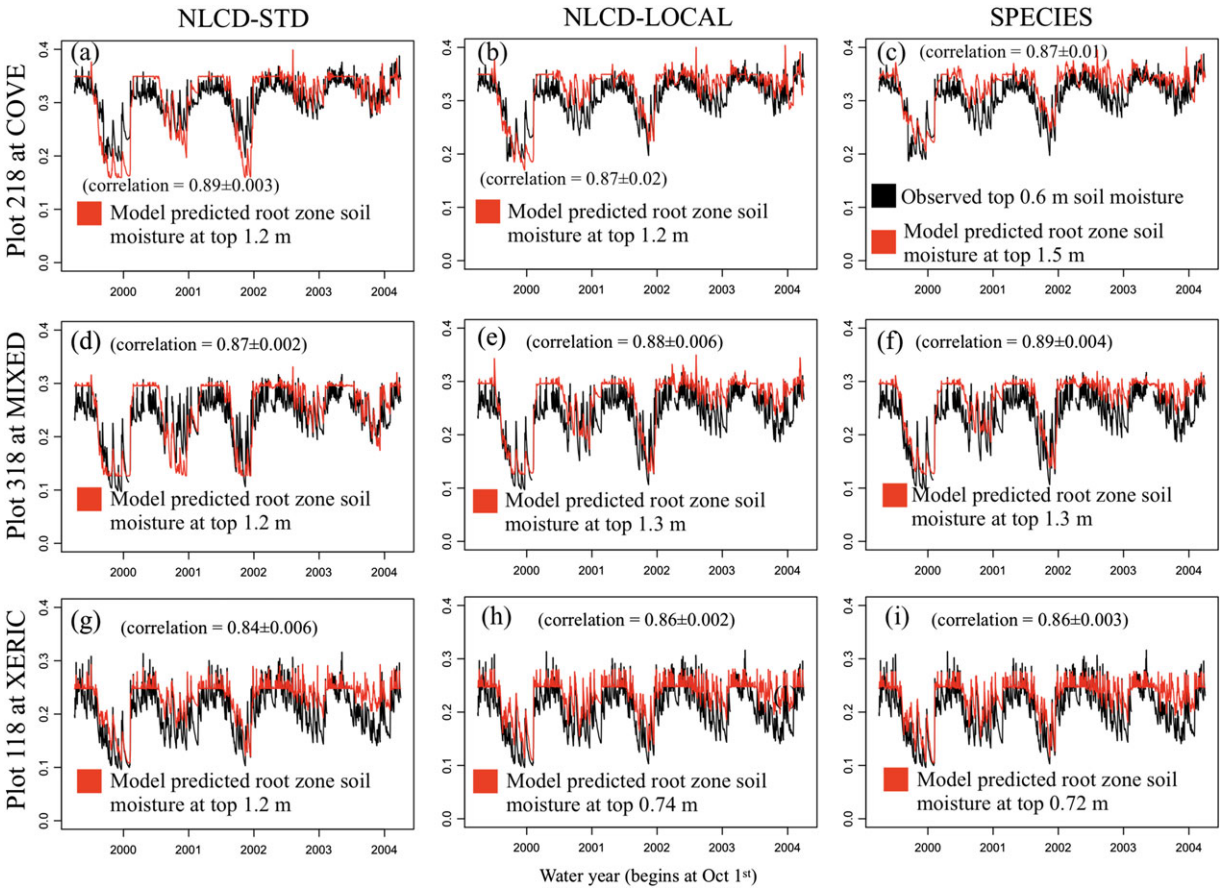

FIGURE 7 Predicted rootzone soil moisture by the three candidate models and the observed 0.6-m soil moisture at three plots in WS18, one plot at each landscape position (i.e., COVE, MIXED, and XERIC)

under a range of conditions. For example, incorporating forest WCT functional organization was hypothesized to better predict flow distribution especially at low flows. This hypothesis was generally supported, as the SPECIES model better fit low flows compared with the other models (Table 2 $NSE_{1/weekly\ flow}$; Figure 4c,d). Additionally, incorporation of canopy WCT functional organization had a significant influence on canopy ecohydrologic behaviour, especially on landscape patterns. The SPECIES model fit observed seasonal patterns of run-off more consistently, beyond what is achieved by separate calibration. The better fit by SPECIES model is due to three major reasons. First, a more realistic evergreen:deciduous ratio in the SPECIES model with the addition of the evergreen understorey compared with the two NLCD models. Oishi et al. (2018) have shown that evergreen understorey at Coweeta Basin contributes significantly to the annual ET, and high density of evergreen understorey under mature deciduous forest area is quite common at the southern Appalachian Mountains (Bolstad et al., 1998). Second, the impact of the accumulated soil moisture deficit during the growth season which conditions the required soil water recharge required for peak flows during the dormant season. Third, WCT spatial organization gives spatial difference in leaf conductance (Table 3), which further results in spatial difference in soil moisture storage and release. Available soil moisture follows a general pattern of increasing downslope following surface and subsurface drainage, modified by soil, slope, and vegetation, which provides a moisture and dissolved nutrient subsidy to hollow and riparian areas, and promoting leaf area increases downhill (Hwang et al., 2009; Mackay & Band, 1997). Simulated ET and productivity show increasing trends downslope, particularly in dry years, following the hypothesis on the downslope subsidy. Tree species that vary in physiologic WCT tend to be patterned by landscape position, covarying with soil moisture and leaf area (Naithani et al., 2013).

In a wet year, simulated ET by all models decreased from COVE to XERIC sites, influenced by LAI landscape pattern (Figure 5a–c). Under dry conditions, differences in available water, water use strategy and stomatal physiology along flowpaths also leads to decreasing ET along COVE to XERIC gradients. However, both NLCD models did not differentiate ET at COVE and MIXED in a dry year, compared with the SPECIES model (Figure 6d–f). In terms of PSN, both NLCD models predicted higher PSN at XERIC than COVE and MIXED in summer (July–September; Figures 5h,i and 6g–i), whereas the SPECIES model maintains higher PSN through the latter portion of the growth season, particularly in the dry year (Figure 6i), which is consistent with observed patterns (Bolstad, Vose, & McNulty, 2001; Hwang et al., 2009). This PSN pattern in the SPECIES model results from better simulated leaf conductance at different landscape positions and its response to soil moisture.

Rootzone soil moisture observed at the COVE site is higher than those at the MIXED and XERIC sites (black lines in Figure 7a,d,g).

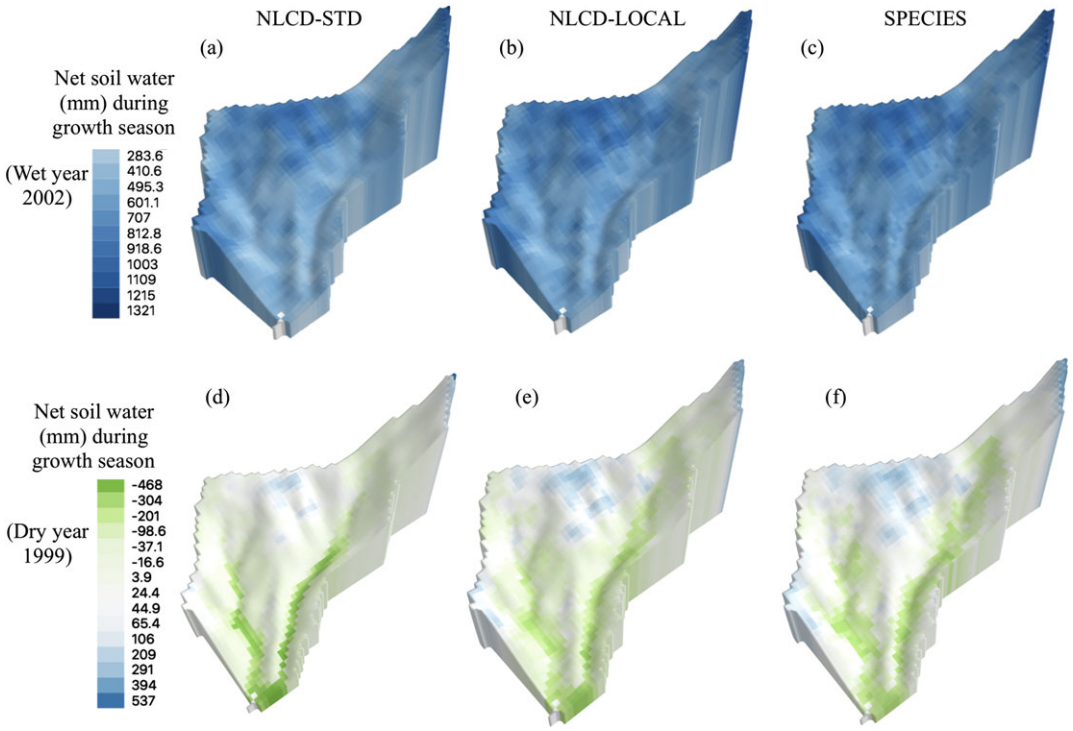

FIGURE 8 Spatial patterns of net soil water (precipitation–evapotranspiration during growth season from April to September) in a wet year (2002) and a dry year (1999) by the three candidate models. Positive net soil water indicates a potential precipitation yielding to downslope through lateral transport. Negative net soil water is the least required soil water recharge from upslope to the current location

TABLE 3 Average net soil water during growth season by three models in wet and dry years

		Leaf conductance during growth season (m s^{-1})		
	Landscape position	NLCD-STD	NLCD-LOCAL	SPECIES
Wet year (2002)	Xeric	693	774	794
	Mixed	580	666	702
	Cove	528	616	633
Dry year (1999)	Xeric	26	65	96
	Mixed	−16	−6	28
	Cove	−70	−74	−98

Note. Positive values indicate that precipitation in excess of local ET, providing surplus exported downslope and to streams. Negative values indicate downslope subsidy of soil water.

TABLE 4 Average leaf conductance during growth season by three models in wet and dry years

	Landscape position	Leaf conductance during growth season (m s^{-1})		
		NLCD-STD	NLCD-LOCAL	SPECIES
Wet year (2002)	Xeric	0.00356	0.00286	0.00209
	Mixed	0.00333	0.00263	0.00230
	Cove	0.00330	0.00258	0.00287
Dry year (1999)	Xeric	0.00265	0.00237	0.00178
	Mixed	0.00214	0.00202	0.00187
	Cove	0.00213	0.00208	0.00247
Percent change from wet year to dry year	Xeric	−25.50%	−17.00%	−14.50%
	Mixed	−35.50%	−23.10%	−18.70%
	Cove	−35.50%	−19.60%	−13.90%

Simulated rootzone soil moisture by all models showed high correlations with observed soil moisture values at the three landscape positions. This is expected with the separately calibrated models using the same LAI and meteorological input data, but the advantage of incorporating canopy WCT functional organization is best reflected in the driest conditions. For example, in dry year (1999), both NLCD models predicted less root zone soil moisture at the COVE than the observed, whereas SPECIES model maintained high root zone soil moisture at the COVE. It is because the SPECIES model simulated better soil moisture patterns with proportionally greater release of moisture for downslope subsidy from upper slope areas, and a more accurate representation of canopy WCT distribution.

Subsurface flowpath moisture redistribution modifies soil water and ET, further affecting hydrologic behaviour, both independently and as it covaries spatially with canopy structure and physiology (Band et al., 1993). For steep watersheds like our study watershed, plant available soil water is higher downslope and lower upslope, as reflected in our models by the decreasing root zone saturation from COVE to XERIC. Previous studies at Coweeta reported higher tree mortality in midslope positions than at downslope and upslope sites during drought (B. Clinton, Boring, & Swank, 1993; B. D. Clinton, Yeakley, & Apsley, 2003), and hypothesized that midslope vegetation is more vulnerable to drought relative to vegetation in upslope and downslope positions, where greater drought adaptation (in upslope) and downslope water subsidies (in downslope) reduce drought effects, respectively. The SPECIES model predicted that MIXED (midslope position) had higher rootzone soil moisture than XERIC (upslope) in a wet year, but rootzone soil moisture dropped as low as XERIC during dry years, while supporting a greater LAI. Correspondingly, the forest productivity (i.e., PSN) at MIXED in the SPECIES model declined to levels comparable to XERIC during summer to early fall. MIXED position shows greater interannual variability in net canopy photosynthesis compared with XERIC and COVE landscape positions. MIXED position also shows the largest declines in leaf conductance in dry compared with wet year (Table 4).

4.2 | Forest structure complexity and WCT organization impacts on forest ecosystem resistance to drought

The importance of forest structural complexity in forest ecosystems has been extensively studied (e.g., Franklin & Van Pelt, 2004; Hardiman, Bohrer, Gough, Vogel, & Curtis, 2011; Hwang et al., 2009). The forest structural complexity, such as the vertical layers of foliage and the horizontal heterogeneity in density and species composition, provides niches for a broad range of organisms, creates microclimates that store energy, water, and nutrients, and mitigate imposed hydroclimate variability on streamflow dynamics (Franklin et al, 1981; Franklin & Van Pelt, 2004; Hardiman et al., 2011). Incorporation of forest structural and compositional complexity could affect modelled watershed-scale emergent behaviour, particularly when exploring ecosystem-level response of forest to disturbance such as drought (Anderegg et al., 2015; Anderegg, Kane, & Anderegg, 2013). In our case, the SPECIES model incorporates some aspects of forest structural complexity by incorporating both an overstorey and understorey vegetation layer (Figure 3). This contributed to its improved performance over the NLCD models because of the larger ET in the SPECIES model in early spring from understorey vegetation in the absence of overstorey shading can significantly influence hydrologic behaviour (Oishi et al., 2018).

Environmental extremes, such as wet and dry years, can impact forest ecosystem processes and a WCT functionally organized forest may be more resistant to such impacts. This hypothesis was supported by our results that the leaf conductance in the SPECIES model showed less and milder reduction between wet and dry years, compared with the two NLCD models (Table 4). The upslope and midslope precipitation surplus provide sufficient subsidy for downslope areas to sustain the cove vegetation during the driest time (Figure 8; Table 3). We suggest this is the result of an "optimization" of WCT functional organization at hillslope scales beyond that of a local patch. Results of our modelled leaf conductance are consistent to those of PSN and rootzone saturation % by landscape location with the midslope forest the most vulnerable to droughts.

Forest WCT functional organization is heavily influenced by climate change, human disturbance and management decisions. In the southern Appalachians, evergreen trees of tracheid xylem (e.g., pines) may dominate if they are planted or germinate by seed after severe soil disturbance (Vose & Ford, 2011), whereas diffuse-porous trees (e.g., tulip poplar and birch) may become dominant after fire suppression, sprouting after forest cutting, or long-term successional dynamics (Caldwell et al., 2016; Elliott, Miniat, Pederson, & Laseter, 2015; Elliott & Swank, 2008). By comparison, ring-porous trees (e.g., oaks) are generally more adapted to drier conditions and fire (Clark et al., 2012; Klos et al., 2009; Vose & Elliott, 2016). Our WCT functional organization modelling approach may help better understand tree species-level spatial variation in controlling catchment-scale hydrologic dynamics, with implications for predicting hydrologic response under climate change and forest management.

4.3 | Implications for ecohydrological modelling

The three models showed relatively small differences in overall goodness of fit to streamflow although the SPECIES model performed slightly better, particularly in dry periods. However, patterns in other ecohydrological parameters, such as rootzone soil moisture and PSN, predicted from the two NLCD models were not consistent with observations and measurements. This suggests that not accounting for spatial patterns in WCT (e.g., forest composition and patterns in NLCD models vs. in SPECIES model) cannot be fully mitigated through numerical calibration, especially in critical dry periods. Fitting to streamflow, and specifically low flow, has been a major focus in evaluation of ecohydrological models. This suggests

caution in using ecohydrologic models that do not account for WCT to examine or interpret changes in other ecohydrologic parameters or simulate ecosystem dynamics other than streamflow.

For our study watershed, species functional group distribution information has been well characterized, but we note that this information will typically be less available in most forest watersheds. However, current advances in remote sensing of biodiversity (e.g., Asner & Martin, 2016; Schimel, Asner, & Moorcroft, 2013) may provide the level of information required to generalize these approaches. As an extension of the present study, we are currently exploring approaches to incorporate canopy WCT functional organization (e.g., using a generalized tree functional group vs. using multiple tree species to represent the canopy) in watersheds with sparse data. Besides using forest WCT and LAI to characterize the heterogeneity of canopy, we should further consider the spatial distribution of xylem anatomy and controls of stem conductance, which are not yet included in this study. Species composition and distribution can be modified through land use change, forest management, and disturbance (Elliott et al., 2015; Vose & Elliott, 2016; Vose & Ford, 2011), and modelling tools such as *RHESSys* that can incorporate species-level information may be useful for guiding management decisions, particularly with regard to forest and water response to future climate scenarios.

5 | CONCLUSIONS

In this study, we presented a modelling framework for incorporating canopy WCT functional organization in watershed-scale hydrology models. We tested the effects of WCT functional organization on catchment-scale ecohydrological behaviour. We demonstrated the importance of WCT functional organization that controls tree water use in partitioning of shallow subsurface flow into transpiration and throughflow along hydrologic flowpaths. We demonstrated the benefit of incorporating this information in a watershed-scale hydrology model. We used the three model structures to address the set of hypotheses pertaining to the watershed-scale function and resistance of the forest ecosystem to drought, with the following conclusions:

1. Canopy WCT functional organization improved model performance not only in terms of the ability to capture observed flow patterns but also in terms of simulating more realistic canopy ecohydrologic behaviour (water and carbon cycling) at hillslope and catchment scales, particularly the impacts of droughts.
2. WCT functional organization conditions the water and nutrient downslope subsidy along the hillslope flowpaths, which is a nonlocal property, and over and above the behaviour of individual patches. Our model results further suggest that forest ecosystem patterns with WCT functional organization are more resistant to drought because of the adjustment of water availability to water demand in the landscape, balanced by the dynamics of downslope subsidy.

ACKNOWLEDGEMENTS

This research was supported by NSF grants supporting the Coweeta Long-Term Ecological Study: DEB-637522, DEB-1440484, DEB-0823923, and NSF CyberSEES CCF-1331813. The U.S. Forest Service provides support for operation of the Coweeta Hydrological Laboratory and access to long-term data.

ORCID

Laurence Lin https://orcid.org/0000-0002-2539-1074
Taehee Hwang https://orcid.org/0000-0002-2755-4279

REFERENCES

Anderegg, W. R., Kane, J. M., & Anderegg, L. D. (2013). Consequences of widespread tree mortality triggered by drought and temperature stress. *Nature Climate Change*, *3*(1), 30–36. https://doi.org/10.1038/nclimate1635

Anderegg, W. R., Schwalm, C., Biondi, F., Camarero, J. J., Koch, G., Litvak, M., … Wolf, A. (2015). Pervasive drought legacies in forest ecosystems and their implications for carbon cycle models. *Science*, *349*(6247), 528–532.

Asner, G. P., & Martin, R. E. (2016). Spectranomics: Emerging science and conservation opportunities at the interface of biodiversity and remote sensing. *Global Ecology and Conservation*, *8*, 212–219. https://doi.org/10.1016/j.gecco.2016.09.010

Band, L. E., Patterson, P., Nemani, R., & Running, S. W. (1993). Forest ecosystem processes at the watershed scale: Incorporating hillslope hydrology. *Agricultural and Forest Meteorology*, *63*(1–2), 93–126. https://doi.org/10.1016/0168-1923(93)90024-C

Bart, R. R., Tague, C. L., & Moritz, M. A. (2016). Effect of tree-to-shrub type conversion in lower montane forests of the Sierra Nevada (USA) on streamflow. *PLoS ONE*, *11*(8), e0161805. https://doi.org/10.1371/journal.pone.0161805

Bolstad, P. V., Swank, W., & Vose, J. (1998). Predicting southern Appalachian overstory vegetation with digital terrain data. *Landscape Ecology*, *13*(5), 271–283. https://doi.org/10.1023/A:1008060508762

Bolstad, P. V., Vose, J. M., & McNulty, S. G. (2001). Forest productivity, leaf area, and terrain in southern Appalachian deciduous forests. *Forest Science*, *47*(3), 419–427.

Bond, B. J., Jones, J. A., Moore, G., Phillips, N., Post, D., & McDonnell, J. J. (2002). The zone of vegetation influence on baseflow revealed by diel patterns of streamflow and vegetation water use in a headwater basin. *Hydrological Processes*, *16*(8), 1671–1677. https://doi.org/10.1002/hyp.5022

Bosch, J. M., & Hewlett, J. (1982). A review of catchment experiments to determine the effect of vegetation changes on water yield and evapotranspiration. *Journal of Hydrology*, *55*(1), 3–23. https://doi.org/10.1016/0022-1694(82)90117-2

Braun, E. L. (1950). *Deciduous forests of eastern North America* (p. 596). New York: McGraw-Hill.

Caldwell, P. V., Miniat, C. F., Elliott, K. J., Swank, W. T., Brantley, S. T., & Laseter, S. H. (2016). Declining water yield from forested mountain watersheds in response to climate change and forest mesophication. *Global Change Biology*, *22*(9), 2997–3012. https://doi.org/10.1111/gcb.13309

Clark, J. S., Bell, D. M., Kwit, M., Stine, A., Vierra, B., & Zhu, K. (2012). Individual-scale inference to anticipate climate-change vulnerability of biodiversity. *Philosophical Transactions of the Royal Society of London*

B: Biological Sciences, *367*(1586), 236–246. https://doi.org/10.1098/rstb.2011.0183

Clinton, B., Boring, L., & Swank, W. (1993). Canopy gap characteristics and drought influences in oak forests of the Coweeta Basin. *Ecology*, *74*(5), 1551–1558. https://doi.org/10.2307/1940082

Clinton, B. D., Yeakley, J. A., & Apsley, D. K. (2003). Tree growth and mortality in a southern Appalachian deciduous forest following extended wet and dry periods. *Castanea*, *68*, 189–200.

Day, F., Phillips, D., & Monk, C. (1988). Forest communities and patterns. In W. T. Swank, & D. A. Crossley, Jr. (Eds.), *Forest hydrology and ecology at Coweeta* (Vol. 66) (pp. 141–149). New York, NY: Springer-Verlag.

Day, F. P., & Monk, C. D. (1974). Vegetation patterns on a southern Appalachian watershed. *Ecology*, *55*(5), 1064–1074. https://doi.org/10.2307/1940356

Dickinson, R. E., Shaikh, M., Bryant, R., & Graumlich, L. (1998). Interactive canopies for a climate model. *Journal of Climate*, *11*(11), 2823–2836. https://doi.org/10.1175/1520-0442(1998)011<2823:ICFACM>2.0.CO;2

Eagleson, P. S. (1982). Ecological optimality in water-limited natural soil-vegetation systems: 1. Theory and hypothesis. *Water Resources Research*, *18*(2), 325–340. https://doi.org/10.1029/WR018i002p00325

Elliott, K. J., Miniat, C. F., Pederson, N., & Laseter, S. H. (2015). Forest tree growth response to hydroclimate variability in the southern Appalachians. *Global Change Biology*, *21*(12), 4627–4641. https://doi.org/10.1111/gcb.13045

Elliott, K. J., & Swank, W. T. (2008). Long-term changes in forest composition and diversity following early logging (1919–1923) and the decline of American chestnut (*Castanea dentata*). *Plant Ecology*, *197*(2), 155–172. https://doi.org/10.1007/s11258-007-9352-3

Elliott, K. J., & Vose, J. M. (2011). The contribution of the Coweeta Hydrologic Laboratory to developing an understanding of long-term (1934–2008) changes in managed and unmanaged forests. *Forest Ecology and Management*, *261*(5), 900–910. https://doi.org/10.1016/j.foreco.2010.03.010

Elliott, K. J., & Vose, J. M. (2012). Age and distribution of an evergreen clonal shrub in the Coweeta Basin: *Rhododendron maximum* L. 1. *The Journal of the Torrey Botanical Society*, *139*(2), 149–166. https://doi.org/10.3159/TORREY-D-11-00076.1

Elliott, K. J., Vose, J. M., Swank, W. T., & Bolstad, P. V. (1999). Long-term patterns in vegetation-site relationships in a southern Appalachian forest. *Journal of the Torrey Botanical Society*, *126*, 320–334. https://doi.org/10.2307/2997316

Eyre, F. H. (1980). *Forest cover types of United States adn Canada* (p. 148). Washington, DC: Society of American Foresters.

Ford, C. R., Elliott, K. J., Clinton, B. D., Kloeppel, B. D., & Vose, J. M. (2012). Forest dynamics following eastern hemlock mortality in the southern Appalachians. *Oikos*, *121*(4), 523–536. https://doi.org/10.1111/j.1600-0706.2011.19622.x

Ford, C. R., Hubbard, R. M., & Vose, J. M. (2010). Quantifying structural and physiological controls on variation in canopy transpiration among planted pine and hardwood species in the southern Appalachians. *Ecohydrology*, *4*(2), 183–195.

Ford, C. R., Laseter, S. H., Swank, W. T., & Vose, J. M. (2011). Can forest management be used to sustain water-based ecosystem services in the face of climate change? *Ecological Applications*, *21*(6), 2049–2067. https://doi.org/10.1890/10-2246.1

Franklin, J. F., Cromack, Jr, K., Denison, W., McKee, A., Maser, C., Sedell, J., … Juday, G. (1981). Ecological characteristics of old-growth Douglas-fir forests. Gen. Tech. Rep. PNW-GTR-118. Portland, OR: U.S. Department of Agriculture, Forest Service, Pacific Northwest Forest and Range Experiment Station. 48 p.

Franklin, J. F., & Van Pelt, R. (2004). Spatial aspects of structural complexity in old-growth forests. *Journal of Forestry*, *102*(3), 22–28.

Garcia, E. S., Tague, C. L., & Choate, J. S. (2016). Uncertainty in carbon allocation strategy and ecophysiological parameterization influences on carbon and streamflow estimates for two western US forested watersheds. *Ecological Modelling*, *342*, 19–33. https://doi.org/10.1016/j.ecolmodel.2016.09.021

Gilks, W. R., Richardson, S., & Spiegelhalter, D. (1995). *Markov chain Monte Carlo in practice*. Boca Raton, Florida: CRC press. https://doi.org/10.1201/b14835

Hales, T., Ford, C., Hwang, T., Vose, J., & Band, L. (2009). Topographic and ecologic controls on root reinforcement. *Journal of Geophysical Research*, *114*(F3), 1–17. https://doi.org/10.1029/2008JF001168

Hanan, E. J., Tague, C. N., & Schimel, J. P. (2017). Nitrogen cycling and export in California chaparral: The role of climate in shaping ecosystem responses to fire. *Ecological Monographs*, *87*(1), 76–90. https://doi.org/10.1002/ecm.1234

Hardiman, B. S., Bohrer, G., Gough, C. M., Vogel, C. S., & Curtis, P. S. (2011). The role of canopy structural complexity in wood net primary production of a maturing northern deciduous forest. *Ecology*, *92*(9), 1818–1827. https://doi.org/10.1890/10-2192.1

Harmon, M., Bratton, S., & White, P. (1984). Disturbance and vegetation response in relation to environmental gradients in the Great Smoky Mountains. *Vegetatio*, *55*(3), 129–139. https://doi.org/10.1007/BF00045013

Hawthorne, S., & Miniat, C. F. (2016). Topography may mitigate drought effects on vegetation along a hillslope gradient. *Ecohydrology*, *11*, e1825. https://doi.org/10.1002/eco.1825

Hewlett, J. D., & Hibbert, A. R. (1963). Moisture and energy conditions within a sloping soil mass during drainage. *Journal of Geophysical Research*, *68*(4), 1081–1087. https://doi.org/10.1029/JZ068i004p01081

Homer, C. G., Dewitz, J. A., Yang, L., Jin, S., Danielson, P., Xian, G., … Megown, K. (2015). Completion of the 2011 National Land Cover Database for the conterminous United States-Representing a decade of land cover change information. *Photogrammetric Engineering and Remote Sensing*, *81*(5), 345–354.

Hwang, T., Band, L., & Hales, T. (2009). Ecosystem processes at the watershed scale: Extending optimality theory from plot to catchment. *Water Resources Research*, *45*(11), W11425.

Hwang, T., Band, L. E., Hales, T., Miniat, C. F., Vose, J. M., Bolstad, P. V., … Price, K. (2015). Simulating vegetation controls on hurricane-induced shallow landslides with a distributed ecohydrological model. *Journal of Geophysical Research – Biogeosciences*, *120*(2), 361–378. https://doi.org/10.1002/2014JG002824

Hwang, T., Band, L. E., Vose, J. M., & Tague, C. (2012). Ecosystem processes at the watershed scale: Hydrologic vegetation gradient as an indicator for lateral hydrologic connectivity of headwater catchments. *Water Resources Research*, *48*(6), W06514.

Jarvis, P. G., & McNaughton, K. (1986). Stomatal control of transpiration: scaling up from leaf to region. *Advances in Ecological Research*, *15*, 1–49. https://doi.org/10.1016/S0065-2504(08)60119-1

Klos, R. J., Wang, G. G., Bauerle, W. L., & Rieck, J. R. (2009). Drought impact on forest growth and mortality in the southeast USA: An analysis using Forest Health and Monitoring data. *Ecological Applications*, *19*(3), 699–708. https://doi.org/10.1890/08-0330.1

Laseter, S. H., Ford, C. R., Vose, J. M., & Swift, L. W. (2012). Long-term temperature and precipitation trends at the Coweeta Hydrologic

Laboratory, Otto, North Carolina, USA. *Hydrology Research*, *43*(6), 890–901. https://doi.org/10.2166/nh.2012.067

Lin, L. (2013). Influences of mountainside residential development to nutrient dynamics in a stream network. (PhD), Virginia Tech University, Blacksburg, VA.

Lin, L., Webster, J. R., Hwang, T., & Band, L. E. (2015). Effects of lateral nitrate flux and instream processes on dissolved inorganic nitrogen export in a forested catchment: A model sensitivity analysis. *Water Resources Research*, *51*(4), 2680–2695. https://doi.org/10.1002/2014WR015962

Mackay, D. S., & Band, L. E. (1997). Forest ecosystem processes at the watershed scale: Dynamic coupling of distributed hydrology and canopy growth. *Hydrological Processes*, *11*(9), 1197–1217. https://doi.org/10.1002/(SICI)1099-1085(199707)11:9<1197::AID-HYP552>3.0.CO;2-W

McGinty, D. T. (1976). Comparative root and soil dynamics on a white pine watershed and in the hardwood forest in the Coweeta basin. (PhD), University of Georgia, Athens, GA,

Miles, B., & Band, L. E. (2015). Green infrastructure stormwater management at the watershed scale: Urban variable source area and watershed capacitance. *Hydrological Processes*, *29*(9), 2268–2274. https://doi.org/10.1002/hyp.10448

Naithani, K. J., Baldwin, D. C., Gaines, K. P., Lin, H., & Eissenstat, D. M. (2013). Spatial distribution of tree species governs the spatio-temporal interaction of leaf area index and soil moisture across a forested landscape. *PLoS ONE*, *8*(3), e58704. https://doi.org/10.1371/journal.pone.0058704

Narayanaraj, G., Bolstad, P., Elliott, K., & Vose, J. (2010). Terrain and landform influence on *Tsuga canadensis* (L.) Carriere (eastern hemlock) distribution in the southern Appalachian Mountains. *Castanea*, *75*(1), 1–18. https://doi.org/10.2179/08-049.1

Oishi, A. C., Miniat, C. F., Novick, K. A., Brantley, S. T., Vose, J. M., & Walker, J. T. (2018). Warmer temperatures reduce net carbon uptake, but do not affect water use, in a mature southern Appalachian forest. *Agricultural and Forest Meteorology*, *252*, 269–282. https://doi.org/10.1016/j.agrformet.2018.01.011

Parton, W. J., Schimel, D. S., Cole, C., & Ojima, D. (1987). Analysis of factors controlling soil organic matter levels in Great Plains grasslands. *Soil Science Society of America Journal*, *51*(5), 1173–1179. https://doi.org/10.2136/sssaj1987.03615995005100050015x

Pataki, D. E., & Oren, R. (2003). Species differences in stomatal control of water loss at the canopy scale in a mature bottomland deciduous forest. *Advances in Water Resources*, *26*(12), 1267–1278. https://doi.org/10.1016/j.advwatres.2003.08.001

Pataki, D. E., Oren, R., Katul, G., & Sigmon, J. (1998). Canopy conductance of *Pinus taeda*, *Liquidambar styraciflua* and *Quercus phellos* under varying atmospheric and soil water conditions. *Tree Physiology*, *18*(5), 307–315. https://doi.org/10.1093/treephys/18.5.307

Running, S. W., & Hunt, E. R. (1993). Generalization of a forest ecosystem process model for other biomes, BIOME-BGC, and an application for global-scale models. In J. R. Ehleringer, & C. Field (Eds.), *Scaling physiological processes: Leaf to globe* (pp. 141–158). San Diego, CA: Academic Press. https://doi.org/10.1016/B978-0-12-233440-5.50014-2

Running, S. W., Nemani, R. R., Peterson, D. L., Band, L. E., Potts, D. F., Pierce, L. L., & Spanner, M. A. (1989). Mapping regional forest evapotranspiration and photosynthesis by coupling satellite data with ecosystem simulation. *Ecology*, *70*(4), 1090–1101. https://doi.org/10.2307/1941378

Schimel, D. S., Asner, G. P., & Moorcroft, P. (2013). Observing changing ecological diversity in the Anthropocene. *Frontiers in Ecology and the Environment*, *11*(3), 129–137. https://doi.org/10.1890/120111

Swift, L. W. J., Cunningham, G. B., & Douglass, J. E. (1988). Climatology and hydrology. In W. T. Swank, & D. A. J. Crossley (Eds.), *Forest hydrology and ecology at Coweeta* (pp. 35–55). New York: Springer. https://doi.org/10.1007/978-1-4612-3732-7_3

Tague, C., & Band, L. (2004). RHESSys: Regional Hydro-Ecologic Simulation System—An object-oriented approach to spatially distributed modeling of carbon, water, and nutrient cycling. *Earth Interactions*, *8*(19), 1–42. https://doi.org/10.1175/1087-3562(2004)8<1:RRHSSO>2.0.CO;2

Van Genuchten, M. T., & Nielsen, D. (1985). On describing and predicting the hydraulic properties. Paper presented at the Annales Geophysicae.

Vose, J. M., & Elliott, K. (2016). Oak, fire, and global change in the eastern USA: What might the future hold?

Vose, J. M., & Ford, C. R. (2011). Early successional forest habitats and water resources. *Sustaining Young Forest Communities*, *Managing Forest Ecosystems*, *21*, 253–269. https://doi.org/10.1007/978-94-007-1620-9_14

Vose, J. M., Miniat, C. F., Luce, C. H., Asbjornsen, H., Caldwell, P. V., Campbell, J. L., … Sun, G. (2016). Ecohydrological implications of drought for forests in the United States. *Forest Ecology and Management*, *380*, 335–345. https://doi.org/10.1016/j.foreco.2016.03.025

Waring, R., Landsberg, J., & Williams, M. (1998). Net primary production of forests: A constant fraction of gross primary production? *Tree Physiology*, *18*(2), 129–134. https://doi.org/10.1093/treephys/18.2.129

Webster, J., Morkeski, K., Wojculewski, C., Niederlehner, B., Benfield, E., & Elliott, K. (2012). Effects of hemlock mortality on streams in the southern Appalachian Mountains. *The American Midland Naturalist*, *168*(1), 112–131. https://doi.org/10.1674/0003-0031-168.1.112

White, M. A., Thornton, P. E., Running, S. W., & Nemani, R. R. (2000). Parameterization and sensitivity analysis of the BIOME-BGC terrestrial ecosystem model: Net primary production controls. *Earth Interactions*, *4*(3), 1–85. https://doi.org/10.1175/1087-3562(2000)004<0003:PASAOT>2.0.CO;2

Whittaker, R. H. (1956). Vegetation of the great smoky mountains. *Ecological Monographs*, *26*(1), 1–80. https://doi.org/10.2307/1943577

Wigmosta, M. S., Vail, L. W., & Lettenmaier, D. P. (1994). A distributed hydrology-vegetation model for complex terrain. *Water Resources Research*, *30*(6), 1665–1679. https://doi.org/10.1029/94WR00436

Wolz, K. J., Wertin, T. M., Abordo, M., Wang, D., & Leakey, A. D. (2017). Diversity in stomatal function is integral to modelling plant carbon and water fluxes. *Nature Ecology & Evolution*, *1*(9), 1292–1298. https://doi.org/10.1038/s41559-017-0238-z

SUPPORTING INFORMATION

Additional supporting information may be found online in the Supporting Information section at the end of the article.

How to cite this article: Lin L, Band LE, Vose JM, Hwang T, Miniat CF, Bolstad PV. Ecosystem processes at the watershed scale: Influence of flowpath patterns of canopy ecophysiology on emergent catchment water and carbon cycling. *Ecohydrology*. 2019;e2093. https://doi.org/10.1002/eco.2093